available at www.sciencedirect.com

ScienceDirect

journal homepage: www.elsevier.com/locate/agrformet

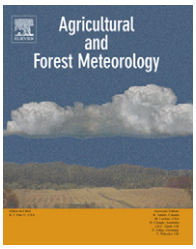

Evaluation of modeled atmospheric boundary layer depth at the WLEF tower

A. Scott Denning [a,*], Ni Zhang [a], Chuixiang Yi [b], Mark Branson [a], Ken Davis [c], John Kleist [a], Peter Bakwin [d]

[a] Department of Atmospheric Science, Colorado State University, Fort Collins, CO 80523, USA
[b] Department of Ecology and Evolutionary Biology, University of Colorado, Boulder, CO 80309, USA
[c] Earth System Science Center, Pennsylvania State University, University Park, PA 16802, USA
[d] NOAA Climate Monitoring and Diagnostics Laboratory, 325 Broadway, Boulder, CO 80305, USA

ARTICLE INFO

Keywords:
Planetary boundary layer (PBL)
WLEF
RUC

ABSTRACT

Accurate simulation of variations in planetary boundary layer (PBL) depth is important for weather prediction and climate studies as well as for carbon cycle analysis. The PBL is difficult to represent in global models because of the need to represent strong gradients associated with capping inversions at arbitrary heights everywhere. Bulk parameterizations of boundary layer processes are therefore an attractive solution. We evaluated a bulk PBL parameterization locally by prescribing horizontal advective tendencies from high-frequency regional meteorological analyses, and running the PBL formulation in a single-column version of a climate model. We compared simulated variations in PBL depth to observations of radar reflectivity and vertical profiles of CO_2 made at a tall tower in northern Wisconsin during 1999. The model captures many features of the observed diurnal and synoptic variability, but tends to underestimate mid-day maxima in PBL depth. Observed late afternoon collapse of the PBL due to decoupling from an underlying stable surface layer is not simulated. The model underestimates mid-day mixing during calm conditions, suggesting underestimation of buoyancy forcing. Conversely, it overestimates PBL depth under windy conditions, suggesting the parameterization is overly sensitive to shear forcing. Global model simulations cannot be compared to specific dates, but monthly mean diurnal cycles show reasonably good agreement to observations at this site. The simulated PBL in the GCM is generally too shallow at mid-day during the summer months, but is well simulated in spring (when it is deeper than summer) and autumn (when it is shallower than in summer). Seasonal rectifier forcing is slightly underestimated by the model at this site.

1. Introduction

The turbulent planetary boundary layer (PBL) mediates the exchanges of heat, water, momentum and carbon between the Earth's surface and the overlying atmosphere. Accurate simulation of the depth of the PBL and the vertical fluxes of momentum and scalar quantities (e.g., energy and water) at the surface and the PBL top are important for numerical weather prediction and climate modeling. Numerical simulation of global or even regional PBL dynamics is challenging because proper representation of surface layer ventilation and turbulent entrainment at the PBL top require very high-vertical resolution of a small fraction of the column. On the other hand, enhanced vertical resolution is "wasted" over most of the daytime mixed

* *Corresponding author.*
E-mail address: denning@atmos.colostate.edu (A.S. Denning).
0168-1923/$ – see front matter © 2007 Elsevier B.V. All rights reserved.
doi:10.1016/j.agrformet.2007.08.012

layer, where gradients of most quantities are small. One can imagine an ideal model structure with many layers close to the surface, one or a very few layers through the mixed layer, many more layers near the PBL top, and relatively coarse layers to represent the overlying free troposphere.

Unfortunately, it is impractical to place ''extra'' layers in a model to represent strong gradients and turbulent entrainment processes, because the height at which these occur varies by more than an order of magnitude. In a global model, the extra layers would need to be simultaneously available 100 m aloft in very stable conditions such as windless nights over ice sheets, in the mid-troposphere over the summer deserts, and everywhere in between. Instead of ''packing'' the bottom half of the simulated atmospheric column with extremely high-vertical resolution (most of which is used to represent weak gradients), an alternative approach is to represent the PBL using a ''zero-order jump model'' with a discontinuity in predicted quantities across its top (e.g., Lilly, 1968; Geisler and Krause, 1969; Tennekes, 1973). Bulk PBL models predict the strength of the capping inversion and the jump in properties as well as the depth of the mixed layer (e.g., Suarez and Arakawa, 1983; Randall et al., 1985, 1989, 1998; Betts, 2000). The advantage of bulk models is that they place the resolution exactly where it is needed (at the variable PBL top), but the disadvantage is that there is no resolution of vertical variations below this level. This approach has recently been extended to a multilayer treatment with a ''stretched'' coordinate that moves with the PBL top (Boezio et al., submitted for publication). Their model retains the advantage of treating the PBL top as a coordinate surface, but allows separate treatment of the surface layer, mixed layer, and entrainment layer and avoiding loss of resolution over the lower troposphere when mixing is very deep.

Seasonal and diurnal variations of PBL depth over land are driven in large part by variations in solar radiation at the surface, which also drives variations in photosynthesis and therefore, net ecosystem exchange (NEE) of CO_2. The common radiative driver of PBL energy and biogeochemistry leads to strong covariance between carbon fluxes and vertical mixing that result in time-mean vertical gradients of CO_2 by a process analogous to an electrical rectifier. The analogy refers to sinusoidal forcing (alternating current/net ecosystem exchange of carbon) being processed (by a diode/diurnal and seasonal cycles of PBL depth) that leads to truncation of the minima in the forcing and produces a ''rectified response (unipolar current/accumulated CO_2 near the surface). Spatial gradients in mixing ratio arising from covariance between NEE and the depth of PBL mixing are a leading source of uncertainty in regional carbon balance derived by tracer transport inversion of atmospheric CO_2 (Denning et al., 1995, 1996, 1999; Law et al., 1996; Law and Raymer, 1999; Gurney et al., 2003).

The WLEF tower site in northern Wisconsin has become the world's first atmospheric ''rectifier observatory.'' It been instrumented for nearly a decade to provide continuous observations of variations in turbulent fluxes of carbon, water, energy, and momentum (e.g., Davis et al., 2003), vertical profiles of wind and scalars throughout and above the surface layer (e.g., Bakwin et al., 1998) and the height of the capping inversion under fair weather conditions (Angevine et al., 1998; Yi et al., 2000, Zhang, 2002). Yi et al. (2004) compared observations of PBL depth and the change in CO_2 across the PBL top from tower and aircraft data to calculations made with the Colorado State University (CSU) General Circulation Model (GCM) (Denning et al., 1996). They showed that the GCM substantially underpredicted the depth of the PBL and the strength of the CO_2 jump at the PBL top. They suggested that the seasonal rectifier effect might actually be stronger than simulated by the CSU GCM, which exhibits this effect more strongly than many other global models used for CO_2 inversions (Law et al., 1996; Gurney et al., 2003). If this result applies generally to temperate land–atmosphere interactions, it would appear to have significant implications for the interpretation of the global carbon budget. Strong rectification in models used for tracer transport inversion requires stronger terrestrial sinks in the northern middle latitudes and (by global mass balance) stronger tropical sources or weaker ocean sinks (Denning et al., 1995, 1999; Gurney et al., 2003).

Interpretation of the rectifier comparison of Yi et al. (2004) is complicated by several mismatches between the simulation and the observations. The radar observations of PBL depth can only be made under fair weather conditions, whereas the GCM simulates all conditions. The large-scale forcing of mean vertical velocity, thermal structure, and surface fluxes is also completely different between the model and the observations, except in the climatological sense, because the GCM does not simulate actual weather events for particular years but rather its own internally consistent weather and biogeochemistry. The PBL depth in the GCM was limited arbitrarily to a maximum fraction of the atmospheric column to prevent attendant loss of vertical resolution. This limit in the GCM merely passes PBL properties associated with very deep mixed layers upward into the next model level, but complicates the comparison with observations.

In this paper, we evaluate simulations of PBL depth in the CSU GCM in more detail. To compare more directly with the observations, we first ran the PBL parameterization from the CSU GCM ''offline,'' in a single-column framework in which we replaced the dependence of column processes on horizontal derivatives with forcing derived from a regional meteorological analysis system. This framework allows us to compare diurnal and synoptic variations in boundary layer depth to radar and tower observations made on specific days. We also compared PBL depth at the appropriate grid cell from a global simulation, but this was only possible in the monthly mean. In the following section, we describe the data we used, the model structure, and the interface to the regional meteorological analysis. In Section 3, we compare the simulated and observed variations of PBL depth over the WLEF site using the single-column model for the summer of 1999, and discuss possible interpretations for the discrepancies between them. We present results of our global simulation in Section 4, and summarize our conclusions and interpretations in Section 5.

2. Methods

2.1. *Observations*

Since 1994, continuous CO_2 mixing ratio measurements have been performed from the WLEF-TV tower at 11, 30, 76, 122, 244

and 396 m by two high-precision Li-COR 6251 CO_2 analyzers (Bakwin et al., 1998). Micrometeorological data and eddy covariance flux have been measured at three levels, 30, 122 and 396 m, since 1996 (Berger et al., 2001; Davis et al., 2003). A radar and radio-acoustic sounding system (RASS) was operated continuously about 8 km east of the tower during two periods from mid-March and the beginning of November in 1998 and 1999 (Angevine et al., 1997; Yi et al., 2001, 2004). The profiler is a 915 mHz Doppler radar, designed to respond to fluctuations of the refractive index in clear air. From the reflectivity of the radar signal, the top of the PBL depth can be determined fairly accurately under good weather conditions. The profiler is very sensitive to large cloud droplets and rain drops so PBL depth cannot be determined during precipitation events or in the presence of fog or low clouds.

The radar profiler is unable to detect features shallower than 400 m above the ground, which limited the measurements of mixed-layer depth to mid-day. The vertical profile of CO_2 mixing ratio observed at six levels on the tower usually exhibited a very strong gradient (5–50 ppm between adjacent levels) in the nocturnal stable layer, with a sharp transition to a weak gradient in the overlying residual layer. We used this transition to identify the top of the stable layer in the data. Following the method of Yi et al. (2001, 2004), we defined the top of the stable surface layer as the midpoint of the uppermost pair of measurement levels for which the difference was greater than a threshold value. We experimented with different thresholds, comparing automatic stable layer detection with visual inspection of the profiles. Vertical variation of CO_2 above the stable layer was usually less than 1 ppm, but infrequent events of short duration required setting a slightly higher threshold. We found that setting the threshold for level-to-level differences to 3 ppm reliably distinguished between the steep gradients in the stable layer and the much weaker gradients aloft. On many mornings, a mixed layer begins to form at the base of the tower (CO_2 mixing ratio differences at adjacent measurement levels of less than 3 ppm) while a stable layer (mixing ratio difference greater than 3 ppm) is still defined on the upper portions of the tower. Under these conditions, we report both a stable layer depth and a mixed-layer depth.

From the radar profiler data, we obtained 35 days of hourly estimates of mixed-layer depth during daytime (11 in July, 12 in August, and 12 in September). We were able to reconstruct nocturnal stable layer (and early morning mixed layer) depths for most nights from the tower CO_2 profiles.

2.2. *Single-column model*

We performed a series of numerical simulations using a single-column model (SCM), which is simply one grid column of the Colorado State University (CSU) General Circulation Model (GCM). The SCM comprises the full GCM "physics", but advective tendencies in temperature, water vapor, and other prognostic quantities that would ordinarily be computed using neighboring grid columns are instead prescribed as "forcing" from another source. This approach allows us to isolate problems with physical parameterizations from other components of the global model. Single-column models have been used as computationally inexpensive testbeds to evaluate cloud models and other physical parameterizations (Randall et al., 1996; Ghan et al., 2000).

The radiation parameterization in the SCM follows Harshvardhan et al. (1987). The cumulus cloud parameterization is based on Arakawa and Schubert (1974), revised with ice phase microphysics (Randall and Pan, 1993), prognostic convective closure, and multiple cloud-base levels (Ding and Randall, 1998). Stratiform clouds (including prognostic cloud droplets, ice crystals, and hydrometeors) are parameterized as described by Fowler et al. (1996) and Fowler and Randall (2002).

The PBL depth is a prognostic quantity in the model and is computed from a mean mass budget:

$$\frac{\partial}{\partial t}\delta p_M = -\nabla\cdot(\mathbf{V}_M\delta p_M) + g(E - M_B)$$

where δp_M is the pressure depth of the PBL, $\mathbf{V}_M$ the PBL wind vector, E the PBL top entrainment rate, and M_B is the net convective mass flux out of the PBL. Changes in the mass of the PBL result from the net large-scale convergence/divergence, the entrainment of air from above the PBL top, and the loss of mass due to convection. The turbulent entrainment rate is calculated from a prognostic equation for the turbulent kinetic energy (TKE), $e = 1/2(\overline{u'^2} + \overline{v'^2} + \overline{w'^2})$, which is obtained by integrating the TKE conservation equation over the depth of the PBL (Randall et al., 1989, 1998; see also Boezio et al., submitted for publication):

$$g^{-1}\delta p_M\frac{\partial e_M}{\partial t} + Ee_M = P - N - D$$

where e_M is the vertically averaged turbulent kinetic energy (TKE), P the gross production of TKE by buoyancy and shear, N is consumption by downward buoyancy fluxes, and D represents dissipation of TKE. The particular definitions of P and N as well as the details of the entrainment rate parameterization can be found in the aforementioned references, but we note here that the entrainment rate is proportional to the square root of the TKE, and is reduced as the PBL-capping inversion becomes sharper. Also, this formulation allows for the entrainment rate to become negative, which is particularly important in the transition from unstable to stable conditions in late afternoon and early evening when PBL "shallowing" typically occurs. Buoyancy and shear production of TKE in the SCM are diagnosed from surface and PBL top fluxes of virtual dry static energy and momentum. Although the global model includes a land-surface parameterization (the simple biosphere model, Sellers et al., 1996), we chose to prescribe the surface fluxes of energy, moisture, and momentum from observations based on eddy covariance measurements (Davis et al., 2003). This allows us to focus on boundary layer physics rather than surface processes in attributing model-data mismatches. The presence of PBL clouds affects the radiative parameterizations, the entrainment rate (through enhanced cloud-top radiative cooling and latent heating), and the exchange of mass with the layer above the PBL as a result of layer cloud instability (Randall, 1987; Randall et al., 1998). If the temperature lapse rate is dry convectively unstable, an adjustment process is initiated that redistributes moisture and enthalpy vertically to restore stability.

The model uses a generalized sigma vertical coordinate (Suarez and Arakawa, 1983) in which the surface is assigned

$\sigma = 2$, the PBL top is assigned $\sigma = 1$, and 100 hPa is assigned $\sigma = 0$ (the model top in the simulations here was set at 51.3 hPa, which was assigned $\sigma = -1$). For $0 < \sigma < 1$, layer boundaries are defined as fractions of the atmospheric mass between 100 hPa and the PBL top. As the surface pressure or the PBL depth change, these ''free troposphere'' layers grow and shrink. When the PBL grows deeper, the free tropospheric mass between the capping inversion and 100 hPa shrinks. In the simulations presented here, we used 17 layers in the vertical: one for the PBL, two ''stratospheric'' layers above 100 hPa, and 14 ''accordion-like'' layers in the free troposphere in between. In global simulations, the boundary layer is limited to 20% of the mass below 100 hPa to prevent loss of resolution in the lower troposphere as PBL mass grows at the expense of upper levels. Yi et al. (2004) noted that predicted mid-day PBL depths were consistently less than observed. For the simulations presented here, we relaxed the limit of maximum PBL depth to 25% of the mass below 100 hPa (about 2 km).

2.3. Regional analyses

We used hourly analyzed weather information from the Rapid Update Cycle (RUC), a high-frequency mesoscale analysis and forecast model system, operated by the National Center for Environmental Prediction (NCEP), to provide lateral boundary forcing for SCM simulations. The RUC assimilates recent observations aloft, such as aircraft data or profilers, and at the surface, such as synoptic data over the United States and surrounding areas, to provide high frequency updates of current conditions and short-range forecasts using a mesoscale weather prediction model (Benjamin et al., 1999). RUC analyses have 40-km horizontal grid spacing, and are run with 40 vertical levels in a hybrid isentropic-sigma coordinate. Available output is interpolated to 37 standard pressure levels. The RUC analyses have the advantage of assimilating high-frequency observations, and are available at much higher frequency than any other operational meteorological product. On the other hand, these are operational analyses, not ''reanalysis'' data as are available for other operational products. They are therefore subject to unpredictable periods of missing data and changes due to updates in the forecast model.

We used the RUC analyses to prescribe horizontal advective forcing to the SCM for the mass, temperature, water vapor, cloud liquid water, cloud ice, and hydrometeors in each model layer. This was done using the flux form of the conservation equation (Randall and Cripe, 1999):

$$\frac{\partial q}{\partial t} = -\left[(\mathbf{V}\cdot\nabla q)_{\text{obs}} + q(\nabla\cdot\mathbf{V})_{\text{obs}} + \frac{\partial}{\partial p}(\omega_{\text{obs}} q)\right] + P$$

$$\omega_{\text{obs}}(p) = -\int_0^p (\nabla\cdot\mathbf{V})_{\text{obs}}\,\mathrm{d}p$$

where q is a prognostic variable, $\mathbf{V}$ the horizontal wind vector, p the pressure, P the production of q and ω is the vertical velocity. Continuous timeseries of RUC analyses were available for four periods: 1–31 July, 15–27 August, 1–9 September and 14–28 September. We performed SCM simulations for each of these periods, and present comparisons of simulated and observed variations in PBL depth in the next section.

2.4. Global model experiment

We performed a 1-year numerical simulation with the global CSU GCM to evaluate the climatology of the simulated depth of the PBL with respect to mean diurnal cycles from the observations. The GCM has changed significantly from the version used by Denning et al. (1996), whose results were analyzed by Yi et al. (2004). The most significant change is the introduction of a completely new dynamical core based on a geodesic grid (Ringler et al., 2000; Randall et al., 2002). The new dynamical core was introduced after the TransCom 3 experiment, so caution should also be used in applying our comparison here to inverse modeling results presented by Gurney et al. (2003). The PBL parameterization remains essentially unchanged, so the comparison to seasonal and diurnal cycles should be applicable within the limits of the overall climate of the model. For consistency with the SCM simulations, we relaxed the limit on PBL depth to 25% of the atmospheric column below 100 mb (as compared to 20% in Denning et al., 1996; Gurney et al., 2003).

Synoptic variations associated with transient weather disturbances should not be interpreted, as the GCM simulation does not represent any specific year. To compare the model simulation to the observations, we sampled the model at the latitude and longitude of the WLEF tower and computed hourly means throughout the year. Monthly means were calculated for each hour of the day after selecting for hours without precipitation, because PBL depth could not be estimated from the radar reflectivity during precipitation events. We compared these selected monthly mean diurnal cycles to means for each hour during 1998 estimated from the radar data as available.

3. Single-column model evaluation

Simulated and observed PBL depths for the entire 3-month period are presented in Fig. 1. Both the model and the observations show a strong diurnal cycle, as expected, and there is substantial day-to-day variability in maximum mixed-layer depth. There are many days for which the observations are only available during the night. Near-surface winds produce shear that favors deeper mixing. Winds were variable throughout the period (Fig. 2), and generally lower in August and September than in July. Winds were relatively calm during several periods (e.g., 10–12 and 17–22 July; 17–21 and 24–25 August; 5–6, 11, 15–16, 20 and 23 September), and the simulated PBL depth tends to be shallower than usual during these periods. Sensible heat flux also promotes mixing via buoyancy forcing. Sensible heat flux showed strong diurnal and synoptic variations (Fig. 3), with daytime maxima usually between 50 and 200 W m^{-2}. Several days exhibited weak winds (shear forcing) and sensible heat fluxes (buoyancy forcing), and consequently the simulated PBL was quite shallow those days (8 and 29 July, 18 August and September 19).

Over the entire period, the model tends to overestimate the PBL depth under stable conditions and to underestimate it under strongly unstable conditions (Fig. 4). The overall comparison of simulated and observed PBL depth reveals three regimes. Much of the time, the model captures the

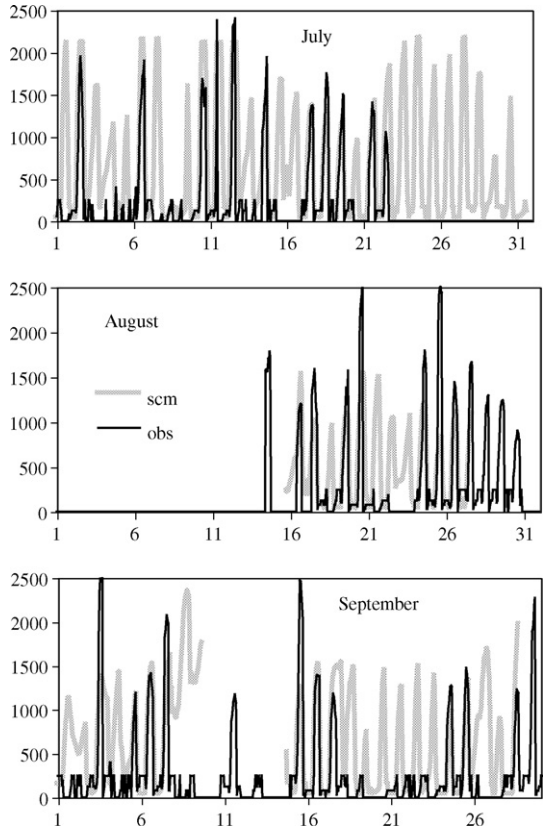

Fig. 1 – Hourly timeseries of simulated (thick gray lines) and observed (thin black lines) PBL depth (m) for July, August, and September of 1999. Observed PBL depth was estimated during daytime from radar reflectivity timeseries for nonprecipitating days when available and from vertical profiles of CO_2 on the tower during stable periods.

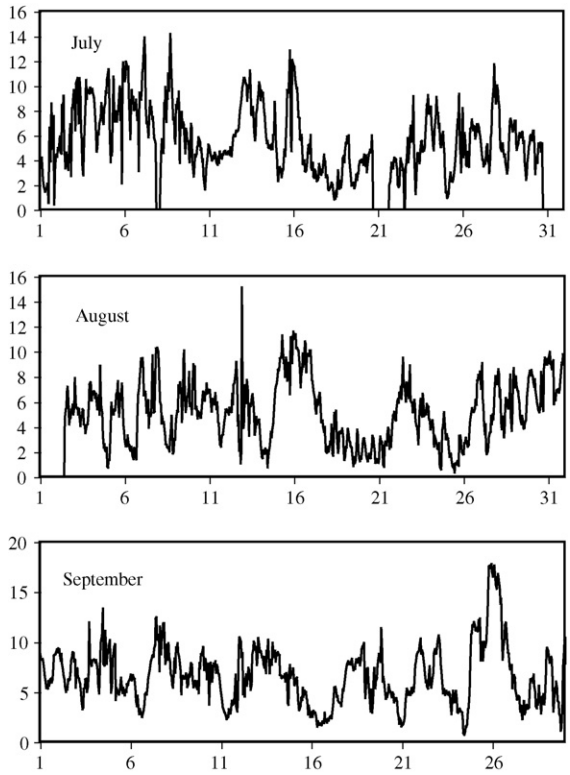

Fig. 2 – Hourly timeseries of wind speed (m s^{-1}) observed at the WLEF-TV tower for July, August and September of 1999. Available measurements made at 30, 122 and 396 m were averaged for each hour.

observed variability fairly well, though there is a tendency to underpredict the mixed-layer depth in the central part of Fig. 4. Another regime is apparent in which the observed PBL is more than 2 km deep, but the SCM simulates a mixed layer of only 800–1500 m depth. A vertical "line" along the right edge of Fig. 4 suggest that the SCM still suffers from "truncation" of PBL depth due to the effects of the limit of PBL depth at 25% of the model atmosphere below 100 hPa (about 2.2 km, see Section 2.2 above). Finally, there are many points along the bottom of Fig. 4 for which the model simulates PBL depths up to 2 km or more, but for which the observations indicate a stable inversion which produces sharp CO_2 gradients seen by the instruments on the tower. The granularity of the measurements can be seen in this regime, with discrete values of observed PBL depth corresponding to instrument placement.

The reasons for some of the various types of model error can be better understood by analyzing monthly mean diurnal cycles of observed and simulated PBL depths (Fig. 5). The observed diurnal cycle is characterized by the rapid growth of the mixed layer during the morning followed by relatively steady values of about 1.5 km all afternoon. There is very little change in observed mid-day mixed layer depth from month to month. The simulated mixed layer begins to form at about the right time, but tends to grow more slowly than in the observations, so that the model underestimates the PBL depth all morning in all months. Mid-day mixed layer depths are well simulated on average in July, but are underestimated in August and September. In those months, the simulated PBL grows steadily from sunrise until the late afternoon. In early evening (19 LT in July, 18 LT in August and 17 LT in September), a stable layer is observed to form, undercutting the mature mixed layer from beneath. This phenomenon cannot occur in the model, due to the bulk representation of the PBL. Mass flows upward by negative entrainment through the coordinate surface that represents the PBL top in the model, but this process is fairly slow, and five or six hours is required to "deflate" the PBL to observed values near midnight. This period in late evening and up to midnight is responsible for the rectangular region of SCM overestimates of PBL depth in Fig. 4. After midnight, the model is quite successful in simulating the very shallow stable layer that is revealed by the gradients of CO_2 observed at the tower. In the morning, these gradients document the formation of a mixed layer that forms below the capping inversion of the nocturnal stable layer. On average, the stable layer persists for 2–3 h after the initiation of shallow mixing at the base of the tower.

Further insight about the model behavior can be gleaned by examining timeseries for particular days (Fig. 6). On three of the days presented (12 and 17 July and 16 September), the

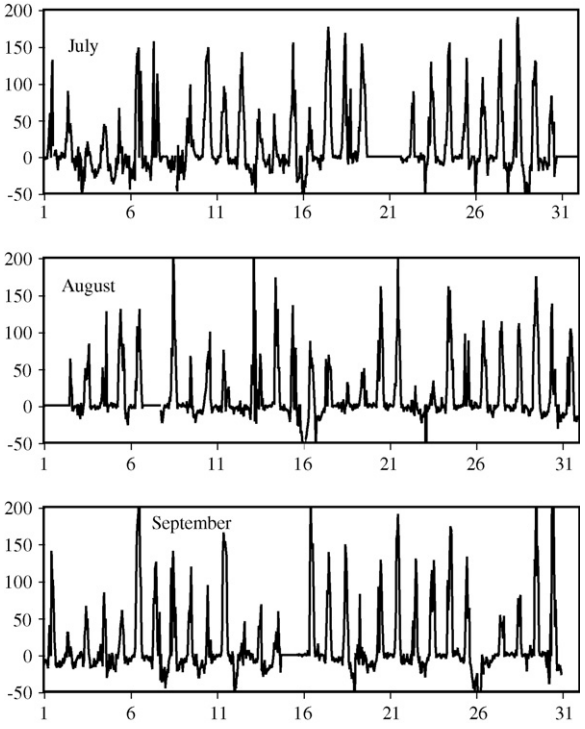

Fig. 3 – Hourly timeseries of surface sensible heat flux (W m^{-2}) computed from eddy covariance measurements corrected for heat storage below each instrument at the WLEF-TV tower for July, August, and September of 1999. Available measurements made at 30, 122 and 396 m were averaged for each hour.

model successfully captures the morning growth and afternoon maximum depth of the mixed layer. On 2 days (20 and 25 August), the model severely underestimates afternoon PBL depth. The synoptic situation on both of these days consisted of high pressure. Both days were exceptionally calm, with mid-day winds in the RUC analyses used to force the SCM less

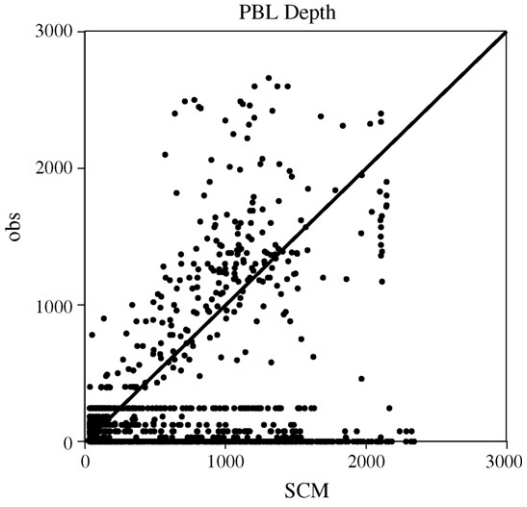

Fig. 4 – Observed vs. simulated PBL depth (m) at each hour for which both a measurement and a simulation were available during the study period. The heavy black line indicates perfect agreement.

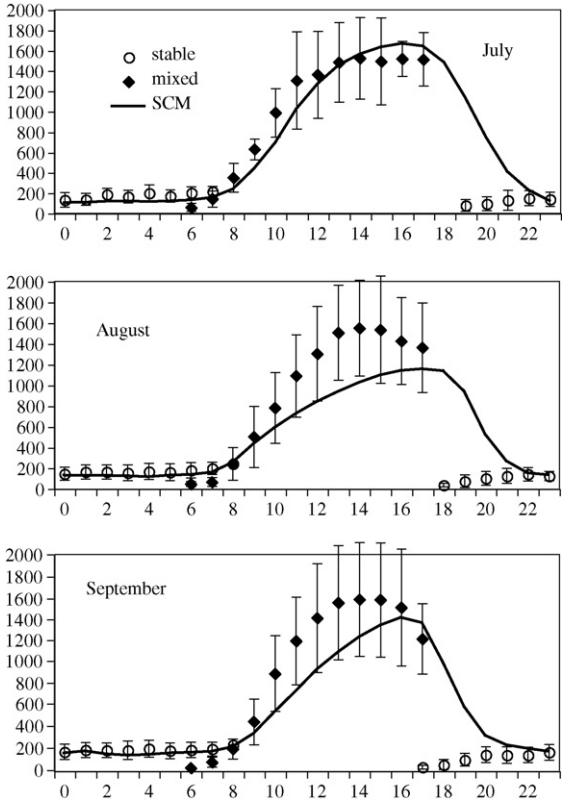

Fig. 5 – Monthly mean diurnal cycles of simulated (heavy line) and observed (symbols) PBL depth (m) at the study site for July, August and September 1999. Observed mixed layer was estimated from radar reflectivity when available, and from vertical profiles of CO_2 measured at the tower in early morning. Stable layer depths were estimated from CO_2 profiles. Error bars indicate the standard deviation of the daily values at each hour. Simulated PBL depths were averaged over nonprecipitating hours to match the sampling limitation of the radar.

than 2 m s^{-1} on 20 August and less than 1 m s^{-1} on 25 August, yet the observed mixed layer was more than 2.5 km deep as documented by the radar. By contrast, the simulated mixed layer is too deep on the afternoons of 2 July and 22 July. On both of those days, the radar indicated the PBL became progressively shallower through the afternoon whereas the model PBL deepened or remained deep. Maximum sensible heat flux was not anomalous on any of these 4 days. Both of these afternoons were characterized by increasing winds, and both were followed by warm frontal passages and rain overnight. Although advective effects are in principle accounted for through the analyzed lateral boundary forcing, it is possible that synoptic forcing played a role in the observations that was not correctly represented in the model. The tendency of the model to underestimate mid-day PBL depth on calm days and overestimate it on windy days suggests that the SCM boundary layer parameterization is overly sensitive to shear forcing.

Finally, on 17 September, the observations indicate a fairly ordinary fall day with a maximum mixed layer depth of about 1300 m shallowing to about 900 m in late afternoon and the

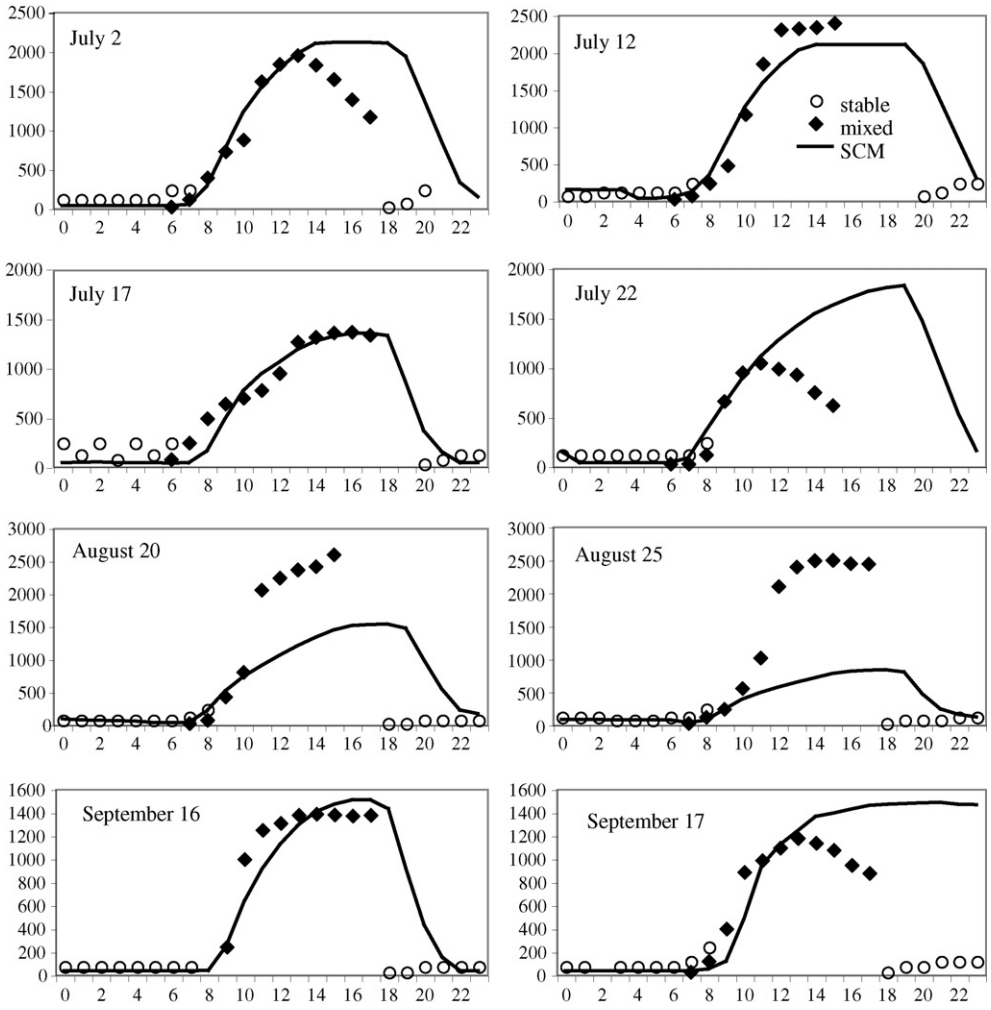

Fig. 6 – Simulated (heavy line) and observed (symbols) variations of PBL depths at the study site for eight specific days during the summer of 1999.

formation of a stable surface layer at 18:00 LT. The model fails to switch into negative entrainment that evening, and the simulated PBL remains about 1400 m deep until the next morning, when it rapidly deflates just before dawn (not shown). This behavior is also noted on the nights of 1–2, 7–8 and 8–9 September (see Fig. 1). On the evening of 17 September, stratiform rain fell in the SCM simulation from about 18 LT until early morning, but no precipitation was observed at the site. Changes in vertical motion and temperature structure associated with this precipitation may be responsible for the failure of the model to generate a stable layer in this case. The synoptic charts for this case show that the region was under high pressure, so incorrect lateral boundary forcing from the RUC analyses is a distinct possibility.

4. Global model evaluation

At the grid cell containing the WLEF tower site, the global model successfully captures the phase of the diurnal cycle of PBL depth (Fig. 7). Mid-day maxima are best captured in April, September, and October, but the GCM systematically underestimates maximum PBL depths by 15–35% during May through August. This period is characterized by lower Bowen ratios of surface fluxes, with weaker buoyancy forcing than during April. The tendency of the model to underestimate changes associated with buoyancy forcing was also noted in the day-to-day variations in the SCM simulations, and may indicate a systematic model deficiency. The observations show very little seasonal variation in maximum PBL depth, with typical values of 1700–2000 m on clear days throughout spring and summer. In September, when net radiation decreases, maximum PBL depths are observed to decrease to about 1500 m, and reach only about 1300 m in October.

Observations of the depth of vertical mixing by PBL turbulence are not available in winter, so quantitative assessment of strength of the seasonal rectifier effect in the GCM is not possible. The simulated carbon flux is a maximum sink in July and a maximum source in October (Denning et al., 1996; Yi et al., 2004). To the extent that these endpoints represent the effects of the entire seasonal cycle, the model slightly underestimates the seasonal rectifier forcing because of its tendency to underestimate mixing during the growing

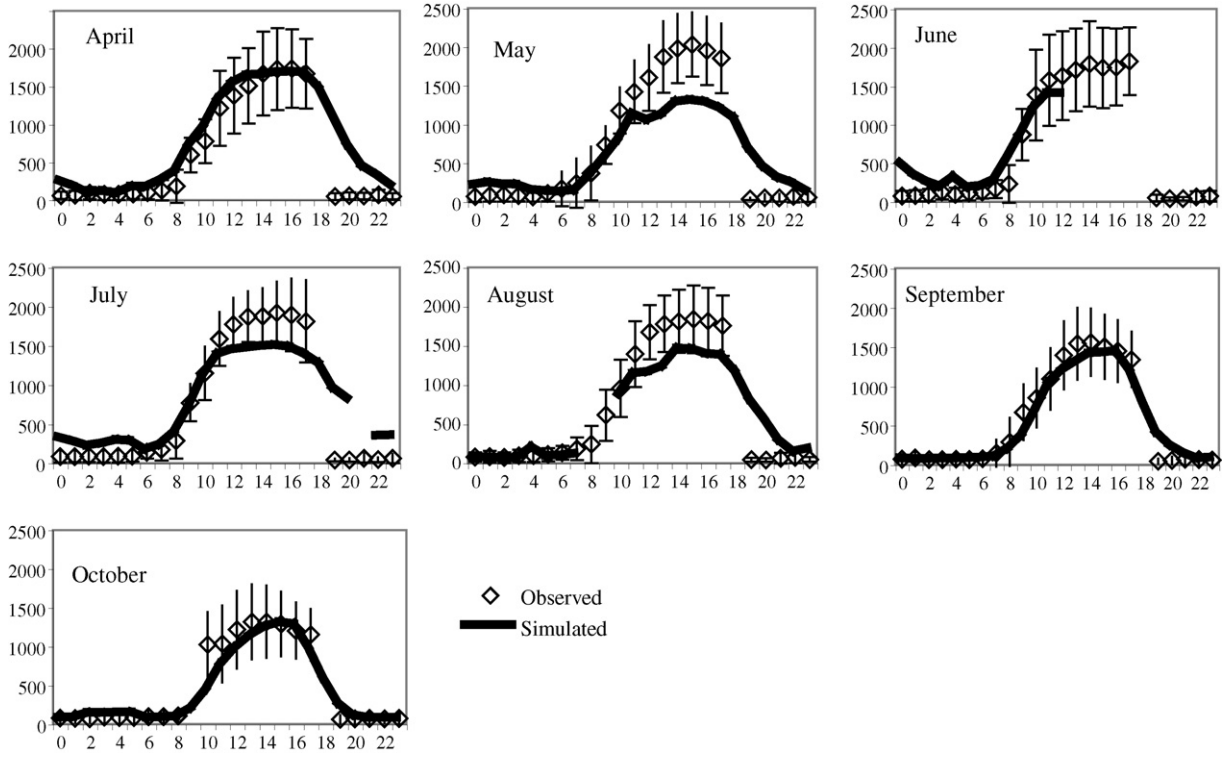

Fig. 7 – Simulated (black line) and observed (open symbols) monthly mean diurnal cycle of PBL depth at the study site. Data are averages of estimated depths of the mixed layer during the day and of the stable layer at night computed from available observations by time of day in 1998. Error bars indicate the standard deviation of the observations for each time. Global simulation was sampled at the WLEF location, and a monthly mean determined for each time of day from hourly means without precipitation. Hours for which fewer than 7 days without precipitation were simulated are not plotted.

season. This interpretation is tenuous however, because it only applies to clear days when the comparison to radar data can be made, and because winter months are not observed. The effect of seasonal rectification on the observed distribution of CO_2 at the remote marine locations of most of the flask stations also depends on the horizontal transport of seasonally stratified air for many thousands of km, so the impact of the slight underestimate of rectifier forcing at this site is difficult to extrapolate to the global CO_2 inversion problem.

5. Discussion and conclusions

We compared the bulk boundary layer model used in the CSU GCM to estimates of PBL depth obtained from observations of radar reflectivity and vertical gradients of CO_2 in the lowest 400 m of the atmosphere at the WLEF tower. The model captures observed variations in PBL depth on diurnal, synoptic, and seasonal time scales reasonably well, both when forced with regional meteorological analyses for specific days and in free-running global simulations. The depth of the nocturnal stable layer is surprisingly well simulated. Morning growth of the PBL by turbulent entrainment is often slower in the model than in the observations, and the late afternoon collapse of the PBL due to the formation of a stable surface layer cannot be simulated by the bulk model presented here. The adoption of a layered PBL model such as the one proposed by Boezio et al. (submitted for publication) would allow this late-day decoupling phenomenon to be represented.

We note a general tendency to underpredict PBL depth during mid-day, on average, during growing season, but not during spring and fall. The underestimation of mid-day PBL depth is most pronounced on very calm days with strong radiation loading. On some windy days, the single-column version of the model overestimates PBL depth. The underestimation of PBL depth is not nearly as pronounced in the simulations presented here as was found by Yi et al. (2004), probably due to our decision to relax the maximum fraction of the atmospheric column defined as the PBL to 25 from 20%. This choice is quite arbitrary, and has less impact than it might appear because when the model reaches this ''lid'' the PBL simply mixes with the layer above. Taken together, the pattern of slower than observed entrainment growth in morning, underestimation of PBL depth on calm days, overestimation on windy days, and the decrease in PBL depth during the growing season when the Bowen ratio is low suggest that the model systematically underestimates buoyancy forcing of TKE.

Given the importance of accurate simulation of covariance between surface carbon fluxes and PBL mixing for the CO_2 inversion problem, quantitative evaluation of models used for tracer transport inversion should be a high priority. It is unlikely that many models can reproduce the rapid changes and strong diurnal and synoptic variations in PBL depth

observed at WLEF. Most transport models rely on forcing from meteorological analysis only four times per day, with the phase of diurnal variations tied to longitude because analyses are available only at 0, 6, 12 and 18 Greenwich Mean Time. PBL simulations driven by these data likely insufficient to resolve some features of the observations.

Further efforts to quantify the rectifier effect in the real atmosphere are needed, but collocated long-term observations of surface carbon fluxes, PBL depth, and vertical profiles of CO_2 are expensive and difficult to obtain. Quantitative comparisons of model simulations to such observations are also difficult due to sparse meteorological analyses with which to drive local models and the inability of the GCM to simulate specific days. The Atmospheric Radiation Measurement Southern Great Plains site is appropriately instrumented for NEE, CO_2 and PBL depth during convective conditions (Ackerman et al., 2004), though without a very tall tower stable layer depths are unlikely to be well observed. It may be possible to simulate longer experimental periods using nested mesoscale simulations nudged at lateral boundaries. The interactions of NEE, PBL depth, horizontal transport, and CO_2 mixing ratio could be compared using coupled ecosystem atmosphere models at the mesoscale (e.g., Nicholls et al., 2004).

Acknowledgements

The work reported here was based in large part on the Master's Degree research of Ni Zhang at Colorado State University, and benefited from long discussions with Dave Randall and Joe Berry. Model development and evaluation work was supported by the Office of Science (BER), U.S. Department of Energy, through both grant number DE-FG02-02EER63474 Amend 03 and through the South Central Regional Center (SCRC) of the National Institute for Global Environmental Change (NIGEC, cooperative agreement TUL-106-00/01 Mod 1). Flux measurements at the WLEF tower were supported in part by the Office of Science (BER), U.S. Department of Energy, through both grant number DE-FG02-03ER63681, and through the Midwestern Regional Center of the National Institute for Global Environmental Change under Cooperative Agreement No. DE-FC03-90ER61010. Mixing ratio measurements at WLEF were supported in part by the Atmospheric Chemistry Project of the Climate and Global Change Program of the National Oceanic and Atmospheric Administration. Boundary layer radar measurements at WLEF were supported in part by the Office of Science (BER), U.S. Department of Energy, grant number DE-FG02-97ER62457, and in part by the instrument deployment pool at the National Center for Atmospheric Research (NSF Atmospheric Sciences). Any opinions, findings and conclusions or recommendations expressed herein are those of the authors and do not necessarily reflect the view of the DOE.

REFERENCES

Ackerman, T.P., Genio, A.D.D., Ellingson, R.G., Ferrare, R.A., Klein, S.A., McFarquhar, G.M., Lamb, P.J., Long, C.N., Verlinde, J., 2004. Atmospheric Radiation Measurement Program Science Plan: Current Status and Future Direcitons of the ARM Science Program, DOE/ER-ARM-0402. U.S. Department of Energy, Office of Biological and Environmental Research.

Angevine, W.M., Bakwin, P.S., Davis, K.J., 1998. Wind profiler and RASS measurements compared with measurements from a 450-m-tall tower. J. Atmos. Oceanic Technol. 15, 818–825.

Arakawa, A., Schubert, W.H., 1974. The interaction of a cumulus cloud ensemble with the large-scale environment, I. J. Atmos. Sci. 31, 674–701.

Bakwin, P.S., Tans, P.P., Hurst, D.F., Zhao, C., 1998. Measurements of carbon dioxide on very tall towers: results of the NOAA/CMDL program. Tellus 50B, 401–415.

Benjamin, S.G., Brown, J.M., Brundage, K.J., Kim, D., Schwartz, B., Smirnova, T., Smith, T.L., 1999. Aviation forecasts from the RUC-2. Preprints. In: Proceedings of the 8th Conference On Aviation, Range, and Aerospace Meteorology. AMS, Dallas, pp. 486–490.

Berger, B.W., Davis, K.J., Yi, C., 2001. Long-term carbon dioxide fluxes from a very tall tower in a northern forest: flux measurement methodology. Am. Meteorol. Soc. 18, 529–542.

Betts, A.K., 2000. Idealized model for equilibrium boundary layer over land. J. Hydrometeorol. 1, 507–523.

Boezio, G.C., Konor, C., Arakawa, A., submitted for publication. A Multi-Layer Bulk PBL Parameterization for Use in Climate Models. Formulation and Application to an Atmospheric General Circulation Model. Submitted to Mon. Wea. Rev.

Denning, A.S., Fung, I.Y., Randall, D.A., 1995. Latitudinal gradient of atmospheric CO_2 due to seasonal exchange with land biota. Nature 376, 240–243.

Denning, A.S., Randall, D.A., Collatz, G.J., Sellers, P.J., 1996. Simulations of terrestrial carbon metabolism and atmospheric CO_2 in a general circulation model. Part 2. Spatial and temporal variations of atmospheric CO_2. Tellus 48B, 543–567.

Denning, A.S., Takahashi, T., Friedlingstein, P., 1999. Can a strong atmospheric CO_2 rectifier effect be reconciled with a "reasonable" carbon budget? Tellus 51B, 249–253.

Ding, P., Randall, D.A., 1998. A cumulus parameterization with multiple cloud-base levels. J. Geophys. Res. 103, 11,341–11,354.

Fowler, L.D., Randall, D.A., 2002. Interactions between cloud microphysics and cumulus convection in a general circulation model. J. Atmos. Sci. 59, 3074–3098.

Fowler, L.D., Randall, D.A., Rutledge, S.A., 1996. Liquid and ice cloud microphysics in the CSU general circulation model. Part 1. Model description and simulated microphysical processes. J. Climate 9, 489–529.

Ghan, S., Randall, D., Xu, K.-M., Cederwall, R., Cripe, D., Hack, J., Iacobellis, S., Klein, S., Krueger, S., Lohmann, U., Pedretti, J., Robock, A., Rotstayn, L., Somerville, R., Stenchikov, G., Sud, Y., Walker, G., Xie, S., Yio, J., Zhang, M., 2000. A comparison of single column model simulations of summertime midlatitude continental convection. J. Geophys. Res. 105 (D2), 2091–2124.

Gurney, K.R., Law, R.M., Denning, A.S., Rayner, P.J., Baker, D., Bousquet, P., Bruhwiler, L., Chen, Y.-H., Ciais, P., Fan, S., Fung, I.Y., Gloor, M., Heimann, M., Higuchi, K., John, J., Kowalczyk, E., Maki, T., Maksyutov, S., Peylin, P., Prather, M., Pak, B.C., Sarmiento, J., Taguchi, S., 2003. TransCom3 CO_2 inversion intercomparison. 1. Annual mean control results and sensitivity to transport and prior flux information. Tellus 55B, 555–579.

Harshvardhan, R.D., Randall, D.A., Corsetti, T.G., 1987. A fast radiation parameterization for atmospheric circulation models. J. Geophys. Res. 92, 1009–1016.

Law, R.M., Raymer, P.J., 1999. Impacts of seasonal covariance on CO_2 inversions. Global Biogeochem. Cycles 13, 845–856.

Law, R.M., Rayner, P.J., Denning, A.S., Erickson, D., Heimann, M., Piper, S.C., Ramonet, M., Taguchi, S., Taylor, J.A., Trudinger, C.M., Watterson, I.G., 1996. Variations in modeled atmospheric transport of carbon dioxide and the consequences for CO_2 inversions. Global Biogeochem. Cycles 10, 783–796.

Lilly, D.K., 1968. Models of cloud-toped mixed layer under strong inversion. Q. J. Roy. Meteorol. Soc. 94, 292–309.

Nicholls, M.E., Denning, A.S., Prihodko, L., Vidale, P.L., Baker, I., Davis, K., Bakwin, P., 2004. A multiple-scale simulation of variations in atmospheric carbon dioxide using a coupled biosphere-atmospheric model. J. Geophys. Res. Atmos. 109 .

Randall, D.A., Cripe, D.G., 1999. Alternative methods for specification of observed forcing in single-column models and cloud system models. J. Geophys. Res. Atmos. 104, 24527–24545.

Randall, D.A., Pan, D.-M., 1993. Implementation of the Arakawa-Schubert cumulus parameterization with a prognostic closure. In: Emanuel, K., Raymond, D. (Eds.), Cumulus Parameterization, Meteorol. Monogr. American Meteorological Society, Boston, Mass, pp. 137–144.

Randall, D.A., Abeles, J.A., Corsetti, T.G., 1985. Seasonal simulations of the planetary boundary layer and boundary-layer stratocumulus clouds with a general circulation model. J. Atmos. Sci. 42, 641–676.

Randall, D.A., Sellers, P., Dazlich, D.A., 1989. Applications of a prognostic turbulence kinetic energy in a bulk boundary-layer model. Atmospheric Science Paper No. 437.

Randall, D.A., Xu, K.-M., Somerville, R.J.C., Iacobellis, S., 1996. Single-column models and cloud ensemble models as links between observations and climate models. J. Climate 9, 1683–1697.

Randall, D.A., Shao, Q., Branson, M., 1998. Representation of clear and cloudy boundary layers in climate models. In: Holtslag, A.A.M., Duynkerke, P.G. (Eds.), Clear and Cloudy Boundary Layers. Roy. Neth. Academic Arts and Science, Amsterdam, pp. 305–322.

Randall, D.A., Ringler, T.D., Heikes, R.P., Jones, P., Baumgardner, J., 2002. Climate modeling with spherical geodesic grids. Comput. Sci. Eng. 4, 32–41.

Ringler, T.D., Heikes, R.P., Randall, D.A., 2000. Modeling the atmospheric general circulation using a spherical geodesic grid: A new class of dynamical cores. Mon. Weather Rev. 128, 2471–2490.

Suarez, M.J., Arakawa, A., 1983. The parameterization of the planetary boundary layer in the UCLA general circulation model: formulation and results. Mon. Weather Rev. 111, 2224–2243.

Tennekes, H., 1973. A model for the dynamics of the inversion above a convective boundary layer. J. Atmos. Sci. 30, 558–567.

Yi, C., Davis, K.J., Berger, B.W., Bakwin, P.B., 2001. Long-term observations of the dynamics of the continental planetary boundary layer. J. Atmos. Sci. 58, 1288–1299.

Yi, C., Davis, K.J., Bakwin, P.S., Denning, A.S., Zhang, N., Desai, A., Lin, J.C., Gerbig, C., 2004. Observed covariance between ecosystem carbon exchange and atmospheric boundary layer dynamics at a site in northern Wisconsin. J. Geophys. Res. 109, D08302 doi:10.1029/2003JD004164.

Zhang, N., Observations and simulations of the planetary boundary layer at a tall tower in northern Wisconsin. M.S. Thesis, Colorado State University, 71 pp.